



Research Paper

An Integrated Geomatics Approach for Projecting Sea Level Variations and Risks A Case Study in the Nile Delta, Egypt¹

Gomaa M. Dawod*, Hala M. Ebaid, Ghada G. Haggag, and
Essam M. Al-Karagy

Survey Research Institute, National Water Research Center, Giza, Egypt

ABSTRACT

Sustainable development of coastal areas depends fundamentally on the availability and comprehensive analysis of precise and up-to-date geospatial datasets. This study aims to develop an integrated geomatics approach for collecting and analyzing heterogeneous datasets within Geographic Information Systems (GIS) environment to predict potential risks of sea level variations over the Nile delta in 2025. Datasets include tide gauge (TG) records span 2008-2018, Global Navigations Satellite System (GNSS) observations to estimate land subsidence and consequently, absolute sea level rise, terrestrial high-accuracy Digital Elevation Model (DEM), and high-resolution satellite imageries were integrated to analyze and evaluate the impact of sea level rise on the coastal area of the Nile delta. Based on the available TG records over five sites, the statistical prediction has been carried out to forecast sea water variations in the next five years over the study area. Next, potentially inundated areas have been delineated for two cases: Mean Sea Level (MSL) and storm surges potential risks (High High water level (HHWL)). The results indicate that the flooded area based on the MSL scenario represents only 5% of the total area of the entire study region, contrasting to earlier un-realistic estimates. Moreover, it has been found that the storm surge case produces potential risks 118% higher than those of MSL. Also, digital maps depicting all possible hazardous areas have been developed. Finally, it can be concluded that the presented integrated approach proves to be significantly effective in risk assessment over the Nile delta, helpful for decision makers to plan actions needed in coastal zone management, and it is reasonable to be applied in other similar regions worldwide.

KEYWORDS: SLR, GNSS, GIS, Geomatics, Risk Assessment

Received 10 August, 2021; Revised: 24 August, 2021; Accepted 26 August, 2021 © The author(s) 2021. Published with open access at www.questjournals.org

I. INTRODUCTION

Sea level rise is essentially attributed to global warming and climate changes factors including ocean thermal expansion, polar ice caps melt, and change in terrestrial storage (e.g. Khan 2019). It is a matter of fact that sea level has been significantly raised in the 20th century on a global average. The Intergovernmental Panel on Climate Change (IPCC) stated that SLR since the mid-19th century has been larger than the mean rate during the previous two millennia (IPCC 2014a). The observed global mean sea rise, from tide gauge records and satellite altimetry data, has been reported as 1.5, 2.0 and 3.2 mm/year for the period 1901-1990, 1971-2010, and 1993-2010 respectively (Church et al. 2013). According to various expected scenarios, the predictable global sea level in 2081-2100, might vary between 0.40 to 0.84 m relative to the 1986-2005 level (IPCC 2019). However, regional SLR rates could be several times larger or smaller than the global mean SLR for periods of several decades, due to fluctuations in ocean circulation, groundwater extraction, and land subsidence among other factors (ibid). Moreover, it has been observed that extreme sea levels (storm surges) have been increased since the last few decades. (ibid). It worth mentioning that due to projected SLR during the 21st century, coastal systems and low-lying regions (such as the river deltas) would increasingly experience strong hazardous impacts (IPCC 2014b).

Hazardous impacts of sea level rise include, for example, shoreline retreat (e.g. Wang et al., 2019), economic impacts on coastal cities (Ruiz-Ramirez et al., 2019), coastal flooding and inundation (e.g. Fu and Peng, 2018), coastal erosion (e.g. Aucelli et al., 2018), decrease in water quality in coastal regions (e.g. Wassef and Schüttrumpf, 2016), decrease in areas and volumes of water bodies (e.g. Hossena and Negm, 2016), and

land degradation (e.g. El Baroudy and Moghanm, 2014). Sea Level Rise (SLR) could be estimated from a variety of techniques and datasets. Relative SLR (RSLR) is primarily measured at Tide Gauge (TG) sites, as well as from satellite altimetry data (e.g. Poitevin et al., 2019). Absolute SLR (ASLR) is a combination of RSLR and land subsidence estimated by levelling or Global Navigation Satellite Systems (GNSS) technique (e.g. Keogh and Törnqvist, 2019). Predicting sea level rise comprises an important task for geodetic and environmental communities

—1 Under review

worldwide (e.g. Siddig et al., 2019). Several mathematical models have been implemented in such a task including ordinary regression (e.g. Dawod et al., 2019), harmonic analysis (e.g. Frota et al., 2016), Artificial Neural Network (ANN) (e.g. Temitope and Daniel, 2014), and moving average filter (e.g. Kaloop et al., 2016). Besides, Geographic Information Systems (GIS) have been widely employed as an integrated framework to investigate and delineate SLR risks (e.g. Neumann et al., 2010).

The Nile delta, Egypt has encountered significant SRL as one of the river deltas and low-lying regions worldwide. Additionally, land subsidence, water and natural gas extraction, and other critical natural aspects heighten vulnerability to coastal flooding and reduce freshwater supply to the delta. A recent study by the IPCC reports that an estimated 2660 km² in the northern delta will be inundated by 2100 for GMSL of 0.44 m. Additionally, subsidence rates range from 0.4 mm/year in the west delta to 1.1 mm/year in the mid-delta and 3.4 mm/year in the east delta (IPCC 2019). The Egyptian government has committed 200 million USD to hard coastal protection at Alexandria and adopted integrated coastal zone management for the northern coast (ibid). In this regard, it worth mentioning that several research studies have stated that Alexandria city in Egypt is considered one of twenty cities worldwide that are most exposed to hazardous natural risks particularly due to coastal flooding by 2070 (Siegel, 2020).

SLR's analysis, prediction, and risk assessment have been extensively investigated in Egypt in the last couple of decades. For example, Dawod et al. (2019) have estimated both relative and absolute sea level rise in the Nile delta region using heterogeneous spatial datasets. GIS has been applied to analyze the sea level rise variations and vital impacts across the Nile delta coasts (Refaat and Eldeberky, 2016, and Mohamed, 2015). Additionally, El-Geziry and Said (2019) have investigated the sea level pattern and variations in El-Burullus new harbor on the Nile delta coastal region. Land subsidence and sea level rise across the Nile delta region have been investigated (e.g. Stanely, 2016). On the other hand, several research studies have been carried out to predict the potential impacts of sea level rise particularly on the Nile delta region (e.g. Hasan et al., 2015 and Hassan and Abdrabo, 2013). Additionally, AlbooHassan et al. (2015) have applied GIS and remote sensing to investigate the sea level rise impacts on coastal tourist services. Hereher (2015) developed a vulnerability index to sea level rise for the Egyptian costs.

Hazardous impacts of sea-water variations are not limited to the gradual SLR but more critically to the dangerous effects of sudden storm surges. A storm surge is an unusual increase of sea water caused by a storm, over and above the predicted astronomical tides. Such an unpredicted rise of the sea water level, due to climate changes, not only has inverse consequences on human life but also the environment, animals, and infrastructural facilities (Rajan and Saud, 2018). For example, on October 2019 the Nile delta and northern parts of Egypt have encountered an unusual type of storm that intimidates to bring forceful seas, tropical-storm strength winds, and probably up to 200 mm of rain to the region. Such rainfall could measure as much as 10 times the average monthly of October across this region, creating a risk of flooding (MODIS 2020). Storm surge is considered a major factor in defining coastal vulnerability over the Mediterranean coasts of Egypt (Torresan et al. 2020). Hence, the investigation of High High Water Level (HHWL) from TG time series would be beneficial in analyzing and defining the potential impacts of storm surges.

The current research study aims to utilize geomatics techniques, particularly TG data, GNSS data, a precise local DEM, GIS, and high-resolution satellite images, in an integrated approach for two objectives: First, to analyze and predict sea level variations (MSL and HHWL) along the Nile delta Mediterranean coasts, Second: to develop a risk assessment of their current and expected potential hazards by 2025.

II. STUDY AREA

The current research focuses primarily on the Nile delta coasts on the Mediterranean sea, ranging from longitude 29.6° E to longitude 32.3° E (Fig. 1). It is worth mentioning that with more than fifty million populations, the Nile delta region might be considered as one of the most densely populated regions worldwide. The topography of the study area (Fig.1) ranges from elevation -72 meter to 197 meters, with an average of 5.9 meters. The dominant elevation is less than 10 meters in the northern and middle parts of the delta. Additionally, it can be realized that the northern region of the delta area has an elevation of less than almost 5 meters. The actual study area extends in the east-west direction over 273 kilometers from Port Said at the east to Alexandria

at the west, with approximately more than one kilometer perpendicular to the shoreline. The overall area of that region equals about 317 square kilometers.

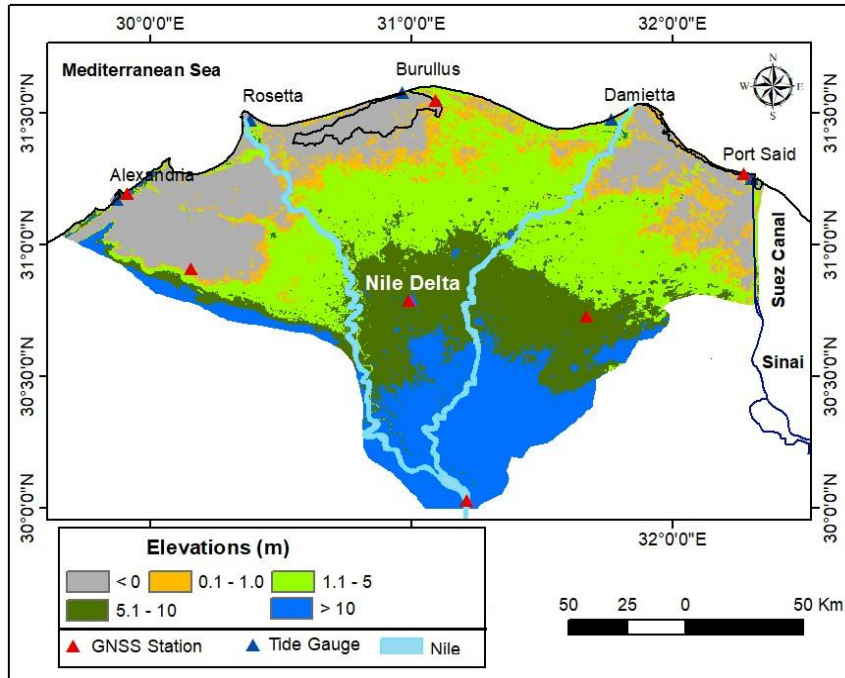


Fig. 1: Topography of the study area, Tide gauges, and GNSS stations

2.1 Data Sets

The available geospatial datasets comprise TG records for analyzing sea level variations, GNSS data to estimate land subsidence, a local high-accuracy DEM to represent the coastal topography, and high-resolution satellite images to delineate the impacts of sea level rise. Those datasets are briefly demonstrated in the next subsections.

2.1.1 Tide Gauge data

Within the Nile delta study area, 5 tide gauge stations exist at Alexandria, Damietta, Burullus, Rosetta, and Port Said (Fig.1). The available tide gauge dataset comprises data from different tide gauge stations along the Mediterranean coasts with variable periods. These tide gauge stations belong to different local organizations, where the Alexandria and Port Said TG stations belong to the Survey Research Institute (SRI) of the National Water Research Center (NWRC), and the other three TG stations belong to the Coastal Research Institute (CoRI) of NWRC.

Table 1 describes the characteristics of the collected tide gauge datasets at these five stations. It should be noticed that the records of the last three TG, in this table, include the annual Mean Sea Level (MSL) and the annual High High Water Level (HHWL) that represents the maximum storm surge at each TG in each year. For the Alexandria and Port Said TG, both MSL and HHWL are estimated from the raw data using arithmetic and statistical functions in the Excel software.

Table 1: Tide Datasets characteristic for Delta coast

TG	Period	Gaps	Frequency
Alexandria	2008 – 2018	No	30 minutes
Port Said	2008 – 2017	No	30 minutes
Damietta	1990 – 2016	1992-1996 2004 – 2011	Yearly
Burullus	2003 – 2016	2010, 2012	Yearly
Rosetta	2004 – 2016	2010, 2012	Yearly

2.1.2 GNSS data

For GNSS monitoring of subsidence in the Nile delta, 24-hours datasets at six stations, covering the period 2012-2015, have been utilized (Mohamed et al., 2015). However; these stations did not cover the Alexandria coast. Therefore; subsidence estimate is acquired for another GNSS station located at Alexandria belong to the "Système d’Observation du Niveau des Eaux Littorales" (SONEL) project, which is international cooperation aims to afford continuous measurements of sea- and land levels at the coast from tide gauges (relative sea levels) and modern geospatial techniques (vertical land motion and absolute sea levels) for studies on long-term sea level trends (SONEL, 2019). That GNSS station is located 3.1 km from the tide gauge. Even though the number of these GNSS stations is relatively small, they have been utilized in this research since they constitute the only available GNSS data for the time being. The previous study revealed comparable results and subsidence rates in the Nile delta region. For example, investigating land subsidence in the Nile delta by satellite radar imageries over 2004-2010, Gebremichael et al. (2018) founded that there exist broad patterns of subsidence (average rate of -2.4 mm/year in the northern delta, almost-steady to small subsidence in the southern delta (average rate of 0.4 mm/year), separated by an uplift zone (average rate of 2.5 mm/year). Similarly, Rateb and Abotalib (2020) utilized Sentinel-1 satellite images over 2015-2019 for monitoring land subsidence in the Nile delta and found that there are three patterns of deformation: land subsides with rates ranging from -12 to -20 mm/year in major cities, subsidence rate ranges between -3 and -8 mm/year along the coastal margins and subsidence rate ranges from -20 to -16 mm/year and -6 to -12 mm/year in newly reclaimed lands on the west and east of the delta's region. The utilized seven GNSS stations are depicted in Figure 1, and their estimated subsidence rates are shown in Table 2. Figure 2 depicts the land vertical movement over the Nile delta region (Dawod et al. 2019).

Table 2 Vertical land movements rates at GNSS stations in the Nile Delta

Station	Period	Subsidence Rate (mm/year)	Reference
Cairo	2012-2015	+ 4.94	Mohamed et al. 2015
Port Said		- 4.72	
Abu Kebeer		+ 3.69	
Tanta		- 6.51	
Baltim		+ 0.71	
Abu El-Matameer		+ 0.55	
Alexandria	2002-2008	-0.85	SONEL 2019

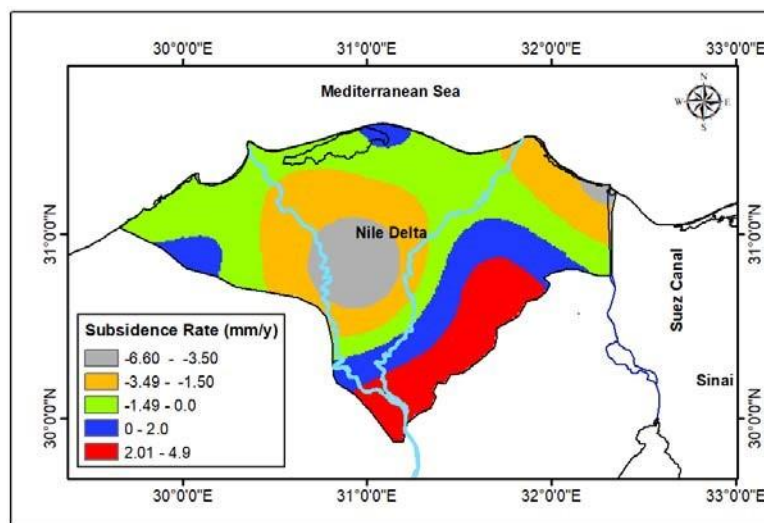


Fig. 2: Vertical land movements in Nile Delta
(ref. Dawod et al. 2019)

2.1.3 Local DEM

Over the study area, terrestrial field campaigns have been performed to develop a local high-precision high-resolution DEM. The utilized field strategy has integrated GNSS measurements with precise levelling. First, a geodetic control network has been established with 5-kilometers spacing. Then, an MSL-based orthometric height for every control point has been determined through precise levelling routes to the nearest Bench Mark (BM). Next, a Post-Processing Kinematic (PPK) GNSS has been implemented in topographic surveying of the entire undeveloped areas. So, about 184 thousand GNSS/Levelling points have been measured. The horizontal spatial resolution of the attained DEM estimated as 1.3 arc seconds, i.e. approximately 40 m, while its vertical accuracy is approximately 0.05 m (SRI 2018). The heights of that accurate DEM range from - 2.035 m to 16.899 m with an average of 1.353 m.

2.1.4 Satellite imageries

TripleSat 1-meter spatial-resolution satellites imageries, dated 2016, have been utilized for land use mapping (Fig. 3). It worth mentioning that the available geospatial datasets applied in the current study have been collected, by SRI, during the period 2016-2018 (SRI 2018). It is a matter of fact that the coastal study area do not include large development projects and it is expected that the existing land uses do not change significantly over recent years. Table 3 showed statistics about the percentage of land uses covering, from which it can be noticed that the undeveloped areas cover almost 70% of the entire study area.



Fig. 3: Land uses at main cities

Table 3: Land uses for the study area

Type	Total Area (km ²)	% of Areas
Undeveloped Areas	221.95	69.9 %
Urban Areas	33.736	10.6 %
Fish Farms	26.579	9.8 %
Agriculture Areas	17.957	6.6 %
Military Areas	8.759	3.2 %

Harbor	4.620	1.7 %
Strait	1.793	0.7 %
Watercourse	1.580	0.6 %
Roads	0.474	0.2 %
Total	317.448	100 %

III. DATA PROCESSING

The approach of processing these integrated data aims to fulfill two objectives: analyzing and predicting sea level variations along the study area, and developing risk assessment of their projected potential hazards by 2025. Consequently, there exist two stages of data processing. First, regression modelling is carried out to analyze and model sea level variations at the utilized TG sites. Although there are several mathematical and statistical methods for modelling and predicting regional or global SLR from TG stations, the linear regression model is one of the most popular ones. It has been applied for such a task in several regions worldwide such as South Korea (Watson 2019), Saudi Arabia (Siddig et al. 2019), and Pacific islands (Martínez-Asensio et al., 2019). The current research study does not concentrate on the comparison of mathematical SLR predicting methods, but rather on developing and applying an integrated geomatics approach for investigating SRL. The linear regression model, utilized herein, has the basic equations in the form of (e.g. Nhan, 2016):

$$MSL(Y) = ax + b \quad (1)$$

where MSL is the annual mean sea level at a tide gauge, a and b are coefficients to be determined, and x is the year.

To judge the attained regression trend, the coefficient of determination, R^2 , is evaluated. It is a statistical measure of the quality of the regression model, representing the proportion of the variance in the dependent variable that is predictable from the independent variable. R^2 ranges from zero to one (or from 0 % to 100 %), computed as:

$$R^2 = \frac{[n \sum xy - (\sum x)(\sum y)]^2}{[n \sum x^2 - (\sum x)^2][n \sum y^2 - (\sum y)^2]} \quad (2)$$

Where n is the number of known data points, x and y are the two dependent and independent variables to be modelled. Generally, the higher R^2 , the better the linear regression model fits the data.

Additionally, studying the storm surges employs another regression analysis using HHWL records at each tide gauge station, as:

$$HHWL(Y) = ax + b \quad (3)$$

The second data processing stage has been performed based on the results of such regression equations (Eq. 1 and 3), for both MSL and HHWL to estimate their projected values for the year 2025. The ArcGIS tools are utilized to delineate and estimate potential inundated regions for these two scenarios (MSL and HHWL). Generally, many spatial interpolation methods exist that may be grouped into three categories: non-geostatistical, geostatistical, and combined techniques. Each method has its merits, disadvantages, and implicit parameters affecting its performance. The kriging geostatistical method, applied in the current study, performs better than non-geostatistical methods and often used in environmental applications (Li and Heap, 2008).

The 16 TripleSat high-resolution satellites images have been georeferenced and adjusted using 58 GNSS Ground Control Points (GCP) . The Erdas remote sensing software has been utilized in such procedure, where the rational polynomial function has been applied. Next, the extraction and classification of land use types have been obtained (SRI 2018). As stated earlier, it is realized that the study area of the current research does not include large current or near-future development planes since it is mainly used for coast guard activities. Therefore, it is expected that the land uses of 2016, as extracted from remote sensing satellite images, will not be altered considerably over the coming few years. Furthermore, such potential flooded areas are

overlaid on the land use map of the study area to assess the possible risks over the Nile delta region. A flowchart of the processing steps is depicted in Figure 4. That process starts by computing the relative SRL, at each station, from tide gauge MSL time series and adding them to the corresponding land subsidence rates to compute the absolute SRL at each TG. Next, the potential MSL in 2025 is computed based on the attained absolute SRL at those locations. Furthermore, a GIS environment has been developed in order to spatially delineate the potential flooded regions based on analyzing the DEM-based topography. Such hazardous regions are then, projected on the land use maps obtained from the processed satellite images. Digital maps and statistical indicators are developed to document the expected MSL risks by 2025. The same steps have been carried out for investigating the high high water level and its potential risks.

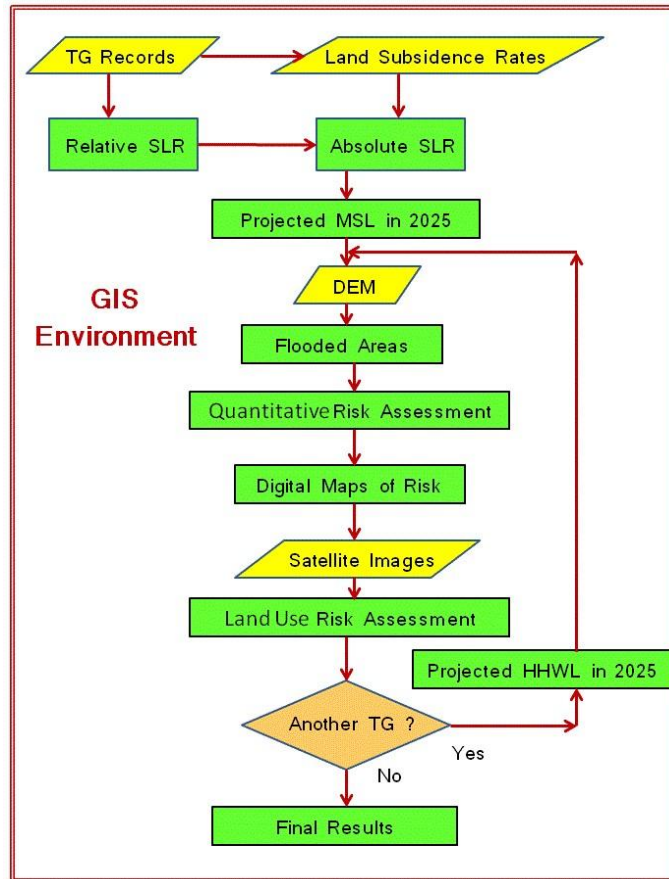


Fig. 4: Data processing flow chart

IV. RESULTS AND DISCUSSIONS

4.1 Results of Sea Level Variations

The results of analyzing the average annual seawater variations at the available five tide gauges are tabulated in Table 4 and were illustrated in Figures 5 and 6. It can be realized that the annual average of MSL range between 0.26 m at Damietta and 0.46 m at Pot Said. It is seen that four TG are close in MSL magnitude while that of Damietta is significantly different. This might be attributed to the long gap of the available dataset at this station. Also, it is noticed that the HHWL varies from 0.88 m at Alexandria to 1.10 m at Rosetta.

Table 4: Statistics of average annual sea water variations at five TG (m) stations

TG	MSL			HHWL
	Minimum	Maximum	Mean	
Alexandria	0.42	0.46	0.45	0.88
Port Said	0.45	0.47	0.46	0.90
Damietta	0.11	0.40	0.26	0.94

Burllus	0.25	0.63	0.41	1.15
Rosetta	0.39	0.46	0.42	1.10

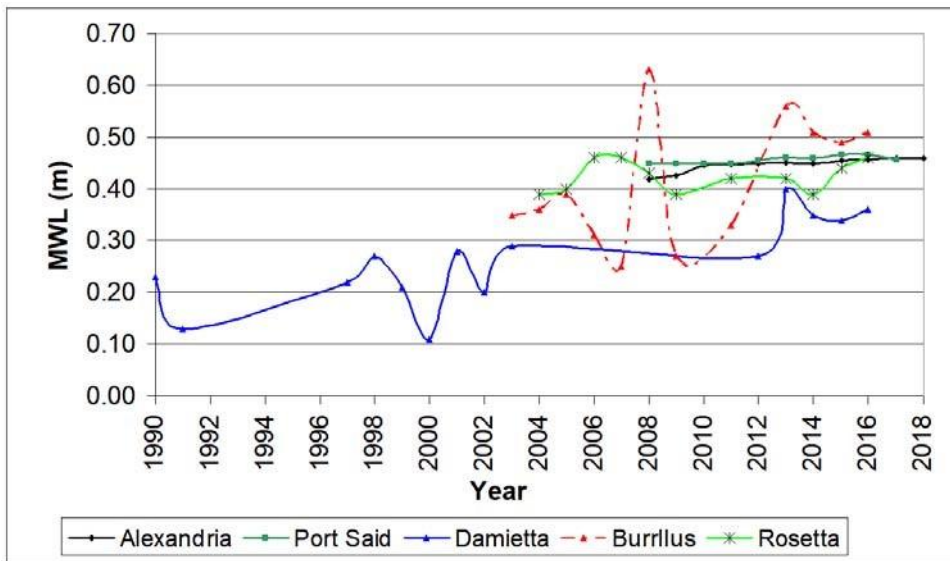


Fig. 5: Mean sea level variations at tide gauges

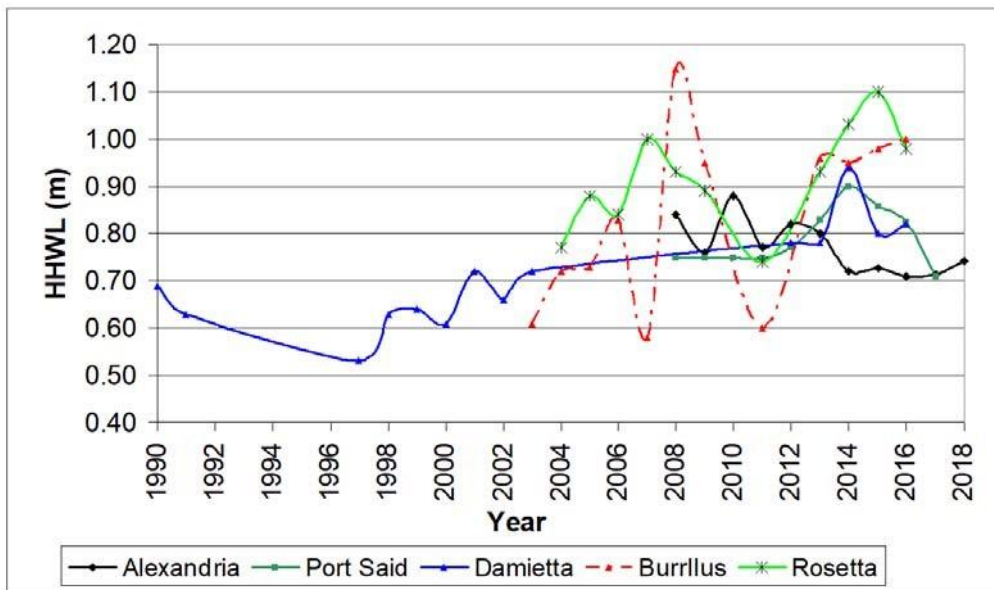


Fig. 6: High High water level variations at tide gauges

Since the available tide dataset contains half-hourly observations at both Alexandria and Port Said, a closer look at tide characteristics is accessible. Figures 7 and 8 depict the average monthly variations of sea water at both gauges over the period 2008-2017. The average monthly MSL at Alexandria ranges from 0.42 m in February to 0.49 m in August. The average HHWL ranges from 0.62 m in March and 0.75 m in August. For Port Said, the average monthly of MSL varies between 0.40 m on April and 0.53 m in August, while the average of HHWL ranges from 0.63 m in February and 0.77 m in September. However, the actual tide observations at these TG over the entire period (2008-2017) reveal that the maximum HHWL reached 0.88 m and 0.90 m at Alexandria and Port Said in August 2010 and March 2014 respectively (Table 5). This indicates that the storm surges could be as much as almost one meter at the Nile delta coasts.

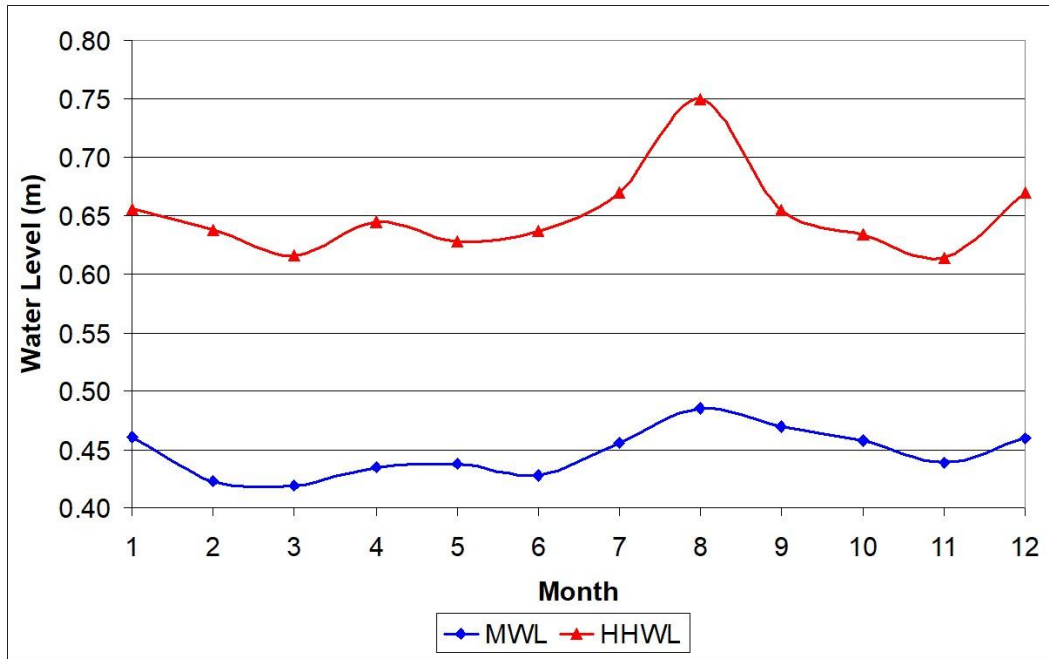


Fig. 7: Average monthly sea level variations at Alexandria TG

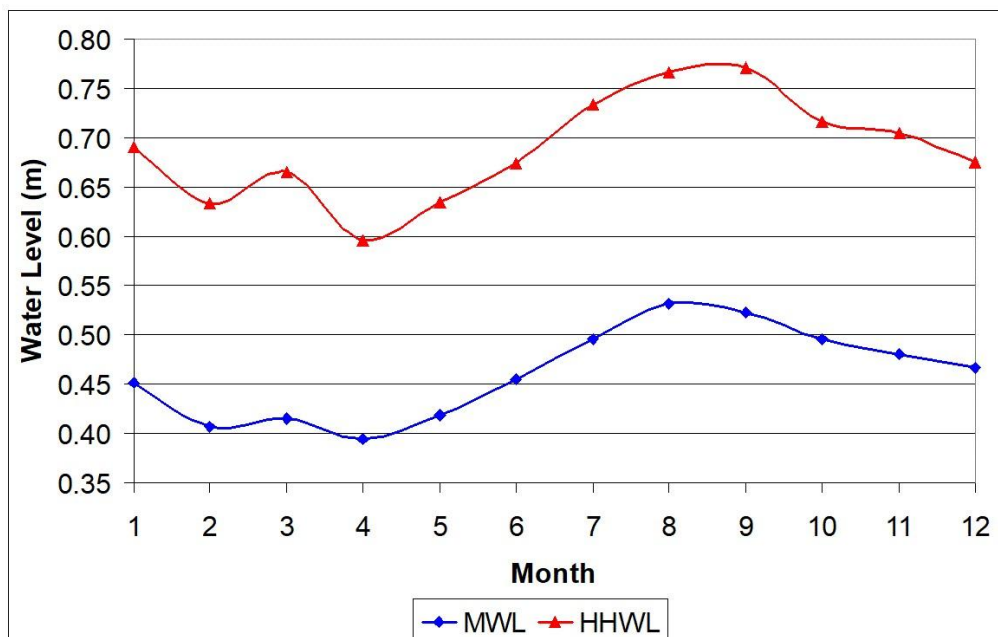


Fig. 8: Average monthly sea level variations at Port Said TG

Table 5: Statistics of actual observed HHWL variations at Alexandria and Port Said TG stations over 2008-2018 (m)

	Minimum HHWL		Maximum HHWL	
	Value (m)	Month	Value (m)	Month
Alexandria	0.46	4/2008	0.88	8/2010
Port Said	0.50	4/2010	0.90	3/2014

Furthermore, the regression analysis (Eq. 1, 3) has been carried out to model MSL and HHWL variations at each TG, along with their corresponding coefficient of determination (R^2) values (Eq. 2). Tables 6 and 7 illustrate the equations for both cases. The applied methodology, herein, depends on investigating the

attained values of R^2 (Tables 6 and 7) as a reasonable indicator for the fit of regression models. Consequently, models of "good" R^2 values are only considered for the prediction of MSL and HHWL potential risks. According to the available data, table 6 demonstrated that the R^2 values of both Burullus and Rosetta TG are very small, which indicates a weak linear regression at these sites based on their available data. Besides, the Damietta TG has a relatively higher trend of annual MSL relative rise (7.4 mm/year) although it lies between Alexandria and Port Said whose annual relative rise equal 3.5 and 1.9 mm/year respectively. Consequently, relative MSL rise rates are only trustable at Alexandria and Port Said TG. Those two rates (Eq. 4 and 5) are employed, next, in projecting sea rise and risk assessment procedures. On the other hand, Table 7 reveals that the regression models of HHWL are only significant for Alexandria and Damietta TG, with considerable R^2 values. That might indicates that, based on the available datasets, HHWL at the available TG sites does not, generally, follow a linear pattern. It worth mentioning that other regression models, such as second-order polynomial, logarithmic model, and exponential model, have been also investigated. However, the attained R^2 indicator of such mathematical models still under 0.40. So, only regression models (Eq. 9 and 11) will be utilized in the potential projection of sea rise and its risk assessment.

Table 6: Statistics of regression analysis of MSL at five TG

TG	Equation	R^2	Eq. No.
Alexandria	$MSL_1 = 0.0035Y + 6.6527$	0.75	4
Port Said	$MSL_2 = 0.0019Y + 3.4118$	0.69	5
Damietta	$MSL_3 = 0.0074Y + 14.643$	0.60	6
Burullus	$MSL_4 = 0.0014Y + 2.4566$	0.04	7
Rosetta	$MSL_5 = 0.0013Y + 2.2609$	0.04	8

Table 7: Statistics of regression analysis of HHWL at Five TG

TG	Equation	R^2	Eq. No.
Alexandria	$HHWL_1 = 0.0124Y + 25.787$	0.52	9
Port Said	$HHWL_2 = 0.0073Y + 13.811$	0.13	10
Damietta	$HHWL_3 = 0.0095Y + 18.419$	0.63	11
Burullus	$HHWL_4 = 0.0235Y + 46.371$	0.32	12
Rosetta	$HHWL_5 = 0.0154Y + 30.022$	0.36	13

Finally, equations 4, 5, 9, and 11 are utilized to predict relative MSL and HHWL estimates in 2025. The projection is limited, herein; to the next five years since the available datasets only cover almost ten years. Next, the land subsidence at each site has been interpolated from Fig. 2, to estimate the absolute sea water rise rates. It has been found the absolute MSL in 2025 equal 0.44 m and 0.46 m at Alexandria and Port Said respectively. Regarding HHWL, it has been found that the projected values at Alexandria and Damietta equal 0.68 m and 0.83 m respectively (Table 8). For other TG stations (with NA values in Table 8), their SLR potential risks in 2025 will be spatially interpolated by GIS.

Table 8: Statistics of projected MSL and HHWL in 2025 (m)

TG	Projected Land Subsidence	Projected MSL		Projected Absolute HHWL
		Relative	Absolute	
Alexandria	0.004	0.435	0.439	0.681
Port Said	0.026	0.436	0.462	NA
Damietta	0.011	NA		0.829

4-2. Results of Sea Level Rise Risk Assessment

Results of projected risk assessment by 2025 in the study area could be divided into two groups: expected constant hazards due to mean sea level rise, and irregular temporal risks due to the storm surge. Findings of both groups are presented in the next sections.

4-2-1. Results of MSL Rise Risk Assessment

Based on the available high-accuracy local DEM, contours zero and 0.45 m have been extracted using the ArcGIS 10 package to delineate potential MSL risks by 2025. It worth mentioning that the value 0.45 m has been used as the average of the projected absolute MSL at both Alexandria and Port Said (Table 8). Accordingly, the spatial area between those two contour lines has been delineated as the potential inundated region, by 2025, due to sea level rise on a mean basis. The area of such a flooded region equals 15.860 Km² that represents only 5% of the total area of the entire study region. This precise finding is crucial for decision makers since some previous estimates of sea level inundated regions have reached as much as few thousands of square kilometers (e.g. Hassaan and Abd-rabo, 2013). That extremely exaggerated differences might be attributed to applying relatively high and unreliable estimates of sea level rise rate (from 0.64 to 2.45 meters by 2100) and the utilization of unaccurate mean for representing the Nile delta topography. It worth mentioning that a high-accuracy DEM has been utilized in the current study, probably for the first time in Egypt, to attain reliable sea rise risk assessment results.

Additionally, it has been noticed that the potential flooded regions do not follow a regular spatial pattern mainly due to the variations in topography. The width of such areas (i.e., the perpendicular direction to the shoreline) ranges from almost 35 meters to 330 meters. Next, the inundated areas have been projected on the land use GIS layer to assess MSL risk on land uses in the Nile delta region. Fortunately, it has been found that 99.9% of the flooded areas exist in undeveloped land use, while the remaining insignificant 0.1% belong to land use of watercourse. Digital maps depicting such hazardous areas have been developed for decision makers and coastal planners.

4-2-2. Results of HHWL Rise Risk Assessment

On the other hand, the accomplished findings of regression analysis showed that the HHWL variations at the utilized TG sites may not follow a linear regression model and its prediction may not be accurate enough. So, the current research investigated two different scenarios as follows. First, the study considered the linear regressions of HHWL at Alexandria and Damietta are "reasonably" good since their R² coefficient are larger than 0.5 (Table 7). So, their projected values in 2025 have been applied to monitor potential future risks. However, since the prediction of the attained regression output is not "very strong", the current research tries another alternative approach. In this regard, the study utilized the maximum recorded HHWL in the available datasets as the worst scenario that could be happened again in the next few years regardless of the expected possible climate changes for the time being. Results of both scenarios are presented, in the next sub-sections, to be considered by decision makers.

Based on the achieved regression model (Eq. 9 and 11), the projected HHWL values at Alexandria and Damietta equal 0.68 m and 0.83 m respectively (Table 8). So, a surface model has been developed by ArcGIS 10 to interpolate expected HHWL in 2025 over the entire study area. Next, the area has been divided into five sub-areas with varying intervals of projected HHWL (Fig. 9). For each sub-area, the potential flooded regions have been delineated. The sum of possible inundated regions due to storm surges (HHWL) is found to be 20.121 km² that represents only 8.23 % of the total study area. It can be realized that the hazards of that projected surge are almost 65% higher than those of the MSL. So, although storm surge is spatiotemporal irregular in nature, its hazardous effects exceed the permanent harmful influences of MSL rise. Moreover, it has been found that the possible flooded regions do not a regular spatial form due to the topography discrepancies. The width of such areas varies between 50 meters and 480 meters approximately. Similarly, the inundated areas have been projected on the land use GIS layer to assess HHWL risk on land uses. Table 9 tabulates the statistics of probable risks on land uses in the study area. Fortunately, it can be seen that 99.68% of the flooded areas exist in undeveloped land use type, while the remaining irrelevant 0.32% belong to other land uses.

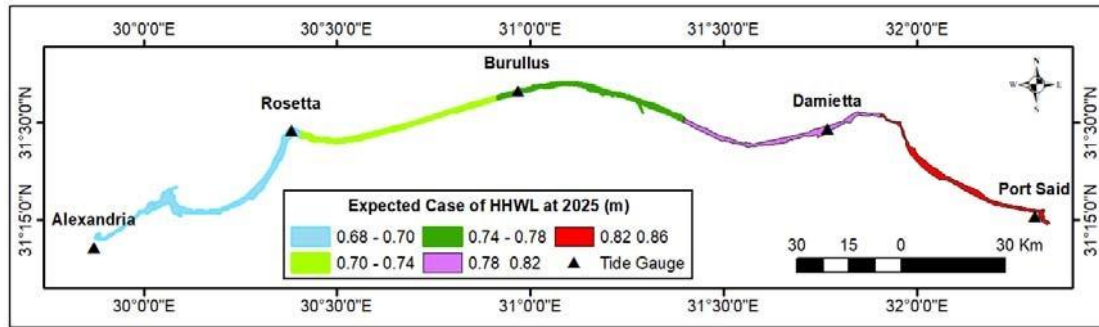


Fig. 9: Variations of expected HHWL in 2025

Second, the worst possible case depends on the potential HHWL of the maximum recorded values in the last decade (last column in Table 4) regardless of any expected possible climate changes for the time being. Another GIS-based interpolation and 3D surface generation have been carried out using those values (Fig. 10). Subsequently, possible inundated regions have been identified over the study area, and the affected land uses have been recognized. It has been found that this HHWL scenario results in flooded regions of a total area of 34.571 km², representing 10.89 % of the study area. That means that this worst scenario of possible storm surge is 32% higher than the mathematically-expected situation, and at the same time, it is 118% higher than the MSL risks. So, storm surges should be noticeably considered by the coastal planners in the Nile delta region. The variable width of such flooded areas ranges between 40 and 1200 meters. Risks of this scenario mainly affect undeveloped areas (by 99.66%), and to a minor extent influence, other land uses (Table 9).

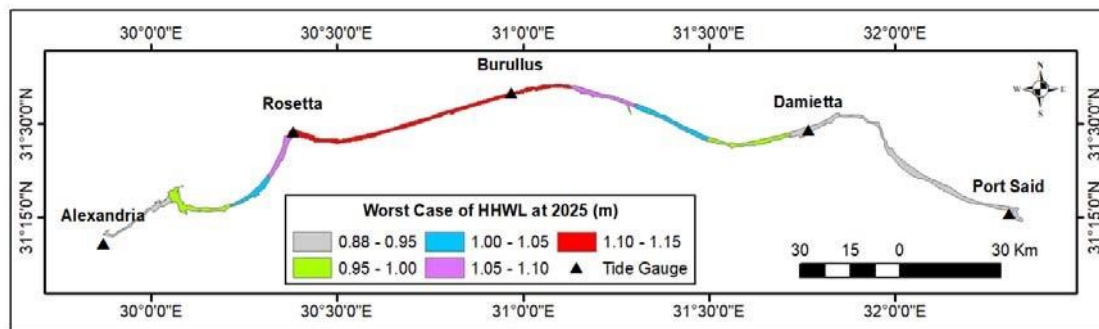


Fig. 10: Variations of worst HHWL in 2025

Table 9: Statistics of two scenarios of surge assessment in 2025

Flooded Land Use	Expected HHWL Scenario		Worst HHWL Scenario	
	Area (km ²)	%	Area (km ²)	%
Undeveloped Areas	26.037	99.68%	34.452	99.66%
Urban Areas	0.066	0.25%	0.029	0.08%
Fish Farms	-	-	0.041	0.12%
Agriculture Areas	0.005	0.02%	0.025	0.07%
Military Areas	-	-	-	-
Harbor	0.006	0.02%	0.0002	0.001%
Strait	0.005	0.02%	0.009	0.03%
Watercourse	0.002	0.01%	0.015	0.04%
Roads	-	-	-	-
Total Area (km ²)	26.121		34.571	
% of Study Area	8.23 %		10.89%	

The utilized precise geospatial datasets, in this study, led to precise estimates of SRL potential risks in the Nile delta region. The main two factors behind such a conclusion is the utilization of accurate national DEM and the determination of reliable estimates of SRL based on national TG stations. Previous studies usually rely on the utilization of global open-source DEM models, which have accuracy levels in the range of three meters in depicting the topography of the Nile delta (Dawod and Al-Ghamdi 2017). A recent study proves that the reliability of such global DEM models in delineating SRL risks is approximately 20% (Abdel-Aziz et al. 2020). Also, previous researches used an unsensible estimate of possible SLR that could reach 2.5 m by 2100 (e.g. Hassaan and Abdrabo 2013). As mentioned in the previous sections, the absolute SLR in the Nile delta is in the range of 0.68 and 0.83 m by the 2025 at Alexandria and Port Said respectively. Results of that study have indicated that approximately 22.5%, 42.2 %, and 49.2 % of the total area of coastal governorates of the Nile delta would be susceptible to inundation under different scenarios of SLR. Similarly, Refaat and Eldeberky (2016) have applied global DEM models (namely GTOPO30 and SRTM) and found that 1401 km² of the Nile delta would be subjected to inundation under SLR of 1.0 m by 2100. Also, Hasan et al. 2015) utilized ASTER and SRTM3 global DEM models and concluded that between 6% and 21% of the Nile delta coastal regions (about 500 km²) would be inundated due to SRL impacts of 0.5 m and 1.0 m respectively by 2100. As a result, it can be concluded that although the global DEM models are free and open-source models for depicting the terrain topography, their utilization in SRL risk assessment could produce insignificant and impractical estimates due to their low vertical accuracy, particularly in low-lying deltaic regions. Hence, acquiring high-accuracy DEM is a vital aspect of SLR risk estimation for coastal management in Egypt and other countries.

V. CONCLUSIONS

Coastal planning and sustainable development rely, on a sense, on the availability of precise up-to-date geospatial information about current and predictable hazards of sea water variations, particularly in low-elevation regions such as river deltas. This research study presented an integrated GIS-based approach, for accomplishing such a fundamental task, comprising tide gauge data, GNSS data, local precise DEM, and high-resolution satellite images. That approach has been carried out, probably for the first time, in the Nile delta region, Egypt as a case study to project the potential sea rise risks in 2025.

The accomplished results indicate that the absolute MSL in 2025 equal 0.44 m and 0.46 m at Alexandria and Port Said respectively, while the projected HHWL at Alexandria and Damietta equal 0.68 m and 0.83 m respectively. On the other hand, findings of projected risk assessment by 2025 could be divided into two groups: expected constant hazards due to mean sea level rise and irregular temporal risks due to the storm surges. The area of such MSL-based flooded region represents only 5% of the total area of the entire study region. Fortunately, it has been found that 99.9% of that flooded areas exist in undeveloped land use, while the remaining insignificant 0.1% belong to land use of watercourse.

Regarding the HHWL-based potential risks, the current research investigated two different scenarios: risk assessment due to the best- attained regression model as the mathematically-expected scenario, and risk assessment due to the worst HHWL situation might happen shortly. For the first scenario, it has been concluded that the sum of possible inundated regions due to storm surges would represent only 8.23 % of the total study area. The GIS-based risk assessment showed that 99.68% of those flooded areas exist in undeveloped land use type. Results of the second HHWL scenario concluded that the inundated regions represent 10.89 % of the study area that means that this worst scenario of possible storm surge is 32% higher than the mathematically-expected situation. Risks of that worst scenario mainly affect undeveloped areas, and to minor extent influence, other land uses. Since HHWL-based potential risks found to be 118% higher than those of MSL, it can be concluded that storm surges should be noticeably considered by the coastal planner in the Nile delta region. It worth mentioning that the accomplished findings prove that the potential impacts of both SRL and surges are significant even though their estimates are significantly less than those of other studies in the literature review. Digital maps depicting all possible hazardous areas have been developed for decision makers and coastal planners. The presented integrated geomatics approach proves to be significantly effective in risk assessment over the Nile delta region, and readable to be applied in other similar regions worldwide.

Declarations:

The authors declare that no funds were allocated for this research

The authors declare that they have no conflict of interest

REFERENCES:

- [1]. Abdel-Aziz T, Dawod G, and Ebaid H (2020) DEMs and reliable sea level rise risk monitoring in Nile Delta, Egypt, Discover Sustainability, V. 1, No. 1, <https://doi.org/10.1007/s43621-020-00006-7>.
- [2]. Alboo-Hassan A, Zidan E, Metwally, Z and Elnaggar A (2015) Changes in coastal line and their impact on coastal tourist services in Damietta governorate, Egypt by Using Remote Sensing and GIS Techniques, Int. J. Eng. Res., 6(7):61-71.

- [3]. Aucelli P, Paola G, Rizzo A, and Rosskopf C (2018) Present day and future scenarios of coastal erosion and flooding processes along the Italian Adriatic coast: the case of Molise region, Environ. Earth Sci., <https://doi.org/10.1007/s12665-018-7535-y>.
- [4]. Church J, Clark P, Cazenave A, Gregory J, Jevrejeva S, Levermann A, Merrifield M, Milne G, Nerem R, Nunn P, Payne A, Pfeffer W, Stammer D and Unnikrishnan A, (2013) Sea Level Change. In: Climate Change 2013: The Physical Science Basis. Contribution of Working Group I to the Fifth Assessment Report of the Intergovernmental Panel on Climate Change [Stocker, T.F., D. Qin, G.-K. Plattner, M. Tignor, S.K. Allen, J. Boschung, A. Nauels, Y. Xia, V. Bex and P.M. Midgley (eds.)]. Cambridge University Press, Cambridge, United Kingdom and New York, NY, USA.
- [5]. Dawod G and Al-Ghamdi K (2017) Reliability of recent global digital elevation models for geomatics applications in Egypt and Saudi Arabia, J. Geogr. Inf. Syst., 9(6):685-698.
- [6]. Dawod G, Mohamed H and Haggag G (2019) Relative and absolute sea level rise based on recent heterogeneous geospatial data: A case study in the Nile delta, Egypt, J. sci. eng , 6(6):55-64.
- [7]. El Baroudy A and Moghamm F (2014) Combined use of remote sensing and GIS for degradation risk assessment in some soils of the Northern Nile Delta, Egypt, Egypt. J. Remote. Sens. Space Sci., <https://doi.org/10.1016/j.ejrs.2014.01.001>
- [8]. El-Geziry T and Said M (2019) Sea level variations in El-Burullus new harbour, Egypt, Arab. J. Geosci, 12:460, <https://doi.org/10.1007/s12517-019-4620-9>.
- [9]. Frota F, Truccolo E and Schettini C (2016) Tidal and sub-tidal sea level variability at the northern shelf of the Brazilian Northeast Region, Anais da Academia Brasileira de Ciências (2016) 88(3): 1371-1386, <https://doi.org/DOI: 10.1590/0001-3765201620150162>.
- [10]. Fu X and Peng Z (2018) Assessing the sea-level rise vulnerability in coastal communities: A case study in the Tampa Bay Region, US, Cities, <https://doi.org/10.1016/j.cities.2018.10.007>
- [11]. Gebremichael E, Sultan M, Becker R, El Bastawesy M, Cherif O and Emil M (2018) Assessing land deformation and sea encroachment in the Nile delta: A radar interferometric and inundation modeling approach, J. Geophys. Res. Solid Earth, 123, 3208–3224. <https://doi.org/10.1002/2017JB015084>.
- [12]. Hassaan M and Abdrabo M (2013) Vulnerability of the Nile Delta coastal areas to inundation by sea level rise, Environ. Monit. Assess., 185:6607–6616, <https://doi.org/10.1007/s10661-012-3050-x>.
- [13]. Hasan E, Khan S and Hong Y (2015) Investigation of potential sea level rise impact on the Nile Delta, Egypt using digital elevation models, Environ. Monit. Assess. 187:649, <https://doi.org/10.1007/s10661-015-4868-9>.
- [14]. Hereher M (2015) Coastal vulnerability assessment for Egypt's Mediterranean coast, Geomatics, Nat. Hazards Risk, 6(4):342–355, <https://doi.org/10.1080/19475705.2013.845115>.
- [15]. Hossena H and Negm A (2016) Change detection in the water bodies of Burullus Lake, Northern Nile Delta, Egypt, using RS/GIS, Procedia Eng., 154:951 – 958.
- [16]. IPCC (2014a) Climate Change 2014: Synthesis Report. Contribution of Working Groups I, II and III to the Fifth Assessment Report of the Intergovernmental Panel on Climate Change [Core Writing Team, R.K. Pachauri and L.A. Meyer (eds.)]. IPCC, Geneva, Switzerland, 151 pp.
- [17]. IPCC (2014b) Climate Change 2014: Impacts, Adaptation, and Vulnerability. Part A: Global and Sectoral Aspects. Contribution of Working Group II to the Fifth Assessment Report of the Intergovernmental Panel on Climate Change [Field, C.B., V.R. Barros, D.J. Dokken, K.J. Mach, M.D. Mastrandrea, T.E. Bilir, M. Chatterjee, K.L. Ebi, Y.O. Estrada, R.C. Genova, B. Girma, E.S. Kissel, A.N. Levy, S. MacCracken, P.R. Mastrandrea, and L.L. White (eds.)]. Cambridge University Press, Cambridge, United Kingdom and New York, NY, USA, 1132 pp.
- [18]. IPCC (2019) IPCC Special Report on the Ocean and Cryosphere in a Changing Climate [H.-O. Pörtner, D.C. Roberts, V. Masson-Delmotte, P. Zhai, M. Tignor, E. Poloczanska, K. Mintenbeck, A. Alegria, M. Nicolai, A. Okem, J. Petzold, B. Rama, N.M. Weyer (eds.)]. In press
- [19]. Kaloop M, Rabah M and Elnabwy M (2016) Sea Level Change Analysis and Models Identification based on Short Tidal Gauge Measurements in Alexandria, Egypt, Mar. Geodesy, <https://doi.org/10.1080/01490419.2015.1134735>.
- [20]. Keogh M and Törnqvist T (2019) Measuring rates of present-day relative sea-level rise in lowelevation coastal zones: a critical evaluation, Ocean Sci., 15:61–73, <https://doi.org/10.5194/os15-61-2019>.
- [21]. Khan A (2019) Why would sea-level rise for global warming and polar ice-melt?, Geosci. Front., 10:481-494, <https://doi.org/10.1016/j.gsf.2018.01.008>.
- [22]. Li J and Heap D (2008) A review of spatial interpolation methods for environmental scientists, Report
- [23]. 2008/23, Geoscience Australia, 137 pp., Australia
- [24]. Martínez-Asensio A, Wöppelmann G, Ballu V, Beckera M, Testuta L, Magnanc A, and Duvata V (2019) Relative sea-level rise and the influence of vertical land motion at Tropical Pacific Islands, Glob Planet Change, 176:132-149.
- [25]. Mohamed H (2015) Spatial analysis of sea level rise in Egypt's northern coast and its influence on the geodetic vertical datum, International Journal of Geomatics and Geosciences, 6(1):45-55.
- [26]. Mohamed H, Shaheen B, Hosney M, and Dawod G (2015) High-precision GPS monitoring of the land subsidence in the Nile Delta: Status and preliminary results, Regional Conference on Surveying and Development, Sharm El-Sheikh, Egypt, Oct. 3-6, 2015.
- [27]. MODIS (Moderate Resolution Imaging Spectroradiometer) (2020) October26, 2019 Rare storm over
- [28]. Mediterranean sea, Available from: https://modis.gsfc.nasa.gov/gallery/individual.php?db_date=2019-10-26, Accessed 18 Dec, 2020.
- [29]. Neumann J, Hudgens D, Herter J and Martinich J (2010) Assessing sea-level rise impacts: A GIS-based framework and application to coastal New Jersey, Coast Manage, 38(4):433-455.
- [30]. Nhan N (2016) Tidal regime deformation by sea level rise along the coast of the Mekong delta, Estuar. Coast. Shelf Sci., (183):382-391.
- [31]. Poitevin C, Wöppelmann G, Raucoules D, Cozannet G, Marcos M and Testut L (2019) Vertical land motion and relative sea level changes along the coastline of Brest (France) from combined space-borne geodetic methods, Remote Sens. Environ., 222:275–285, <https://doi.org/10.1016/j.rse.2018.12.035>.
- [32]. Rajan C and Saud J (2018) Storm surge and its effect - A review on disaster management in coastal area, J. Civ. Eng. Res., 4(5):204-210.
- [33]. Rateb A and Abotalib A (2020) Inferencing the land subsidence in the Nile Delta using Sentinel-1 satellites and GPS between 2015 and 2019, Sci. Total Environ. 729:138868, <https://doi.org/10.1016/j.scitotenv.2020.138868>
- [34]. Refaat M and Eldeberky Y (2016) Assessment of coastal inundation due to sea-level rise along the Mediterranean coast of Egypt, Mar. Geodesy, <https://doi.org/10.1080/01490419.2016.1189471>.
- [35]. Ruiz-Ramirez J, Euan-Avila J and Rivera-Monroy V (2019) Vulnerability of coastal resort cities to mean sea level rise in the Mexican Caribbean, Coast Manage, <https://doi.org/10.1080/08920753.2019.1525260>.

- [36]. Siegel F (2020) Adaptations of Coastal Cities to Global Warming, Sea Level Rise, Climate change and endemic hazards, Springer Briefs in Environ. Sci., Switzerland; https://doi.org/10.1007/978-3030-22669-5_7.
- [37]. Siddig N, Al-Subhi A and Alsaafani M (2019) Tide and mean sea level trend in the west coast of the Arabian Gulf from tide gauges and multi-missions satellite altimeter, *Oceanologia*, 61:401— 411.
- [38]. SONEL (Système d'Observation du Niveau des Eaux Littorales) (2019) Available from: <http://www.sonel.org/>, Accessed 22 Jun 2019.
- [39]. Stanley J (2016) Increased land subsidence and sea level rise are submerging Egypt's Nile delta costal margin, *GSA Today*, V. 27, <https://doi.org/10.1130/GSATG312A.1>.
- [40]. SRI (Survey Research Institute) (2018) The final report of the research study of management plan of the costal areas over the Mediterranean sea from Port Said to Alexandria, Internal Report, 199 pp., Egypt.
- [41]. Temitope B and Daniel U (2014) Modelling and Prediction of Water Level for a Coastal Zone Using Artificial Neural Networks, *Int. J. Comput. Eng. Sci.*, 4(6):26-41.
- [42]. Torresan S, Furlan E, Critto A, Michetti M and Marcomini A (2020) Egypt's coastal vulnerability to sea-level rise and storm surge: Present and future conditions, *Integr. Environ. Assess. Manag.*, 16(5):761–772.
- [43]. Wang F, Lia J, Shia P, Shanga Z, Lia Y and Wang H (2019) The impact of sea-level rise on the coast of Tianjin-Hebei, China, *China Geol.*, 1:26–39.
- [44]. Wassef R and Schüttrumpf H (2016) Impact of sea-level rise on groundwater salinity at the development area western delta, Egypt, *Groundw. Sustain. Dev.*, (2-3): 85–103.
- [45]. Watson P (2019) Updated mean sea level analysis: South Korea, *J Coast Res*, 35(2):241-250.